NASA TECHNICAL MEMORANDUM

NASA TM X-71830

NASA TM X-71830

ATTENUATION OF SOUND IN DUCTS WITH ACOUSTIC TREATMENT - A GENERALIZED APPROXIMATE EQUATION

by Edward J. Rice
Lewis Research Center
Cleveland, Ohio 44135

TECHNICAL PAPER to be presented at Ninetieth Meeting
of the Acoustical Society of America
San Francisco, California, November 4-7, 1975

ABSTRACT

A generalized approximate equation for duct lining sound attenuation is presented. The specification of two parameters, the maximum possible attenuation and the optimum wall acoustic impedance is shown to completely determine the sound attenuation for any acoustic mode at any selected wall impedance. The equation is based on the nearly circular shape of the constant attenuation contours in the wall acoustic impedance plane. For impedances far from the optimum, the equation reduces to Morse's approximate expression. The equation can be used for initial acoustic liner design. Not least important is the illustrative nature of the solutions which provide an understanding of the duct propagation problem usually obscured in the exact calculations. Sample calculations using the approximate attenuation equation show that the peak and the bandwidth of the sound attenuation spectrum can be represented by quite simple functions of the ratio of actual wall acoustic resistance to optimum resistance.

E-8540

ATTENUATION OF SOUND IN DUCTS WITH ACOUSTIC TREATMENT - A GENERALIZED APPROXIMATE EQUATION

by Edward J. Rice

Lewis Research Center

SUMMARY

A generalized approximate equation for duct lining sound attenuation is presented. The specification of two parameters, the maximum possible attenuation and the optimum wall acoustic impedance is shown to completely determine the sound attenuation for any acoustic mode at any selected wall impedance. The equation is based on the nearly circular shape of the constant attenuation contours in the wall acoustic impedance plane. For impedances far from the optimum, the equation reduces to Morse's approximate expression.

The equation can be used for initial acoustic liner design. Not least important is the illustrative nature of the solutions which provide an understanding of the duct propagation problem usually obscured in the exact calculations.

Sample calculations using the approximate attenuation equation show that the peak and the bandwidth of the sound attenuation spectrum can be represented by quite simple functions of the ratio of actual wall acoustic resistance to optimum resistance.

INTRODUCTION

The approximate sound attenuation equation developed by Morse (ref. 1) which is valid for nearly hard walls has been extremely useful and produces quite good results over its range of validity. This equation is easy to use requiring only liner resistance, reactance, and duct length to diameter ratio as inputs. Unfortunately, as liner resistance is reduced and the exact calculations using the wave equation predict higher sound attenuations, the approximate equation becomes inaccurate.

The purpose of this paper is to generate an approximate sound attenuation equation which is as simple as possible in form but which will adequately compare with some exact calculations in the lower resistance or high attenuation region of the wall impedance plane. The approximate equation is anchored on the optimum impedance and the maximum possible attenuation associated with

this impedance. This optimum has been extensively studied and reported for single (ref. 2) and multiple modes (ref. 3) without flow, multiple modes with flow (ref. 4), for spinning modes with uniform flow (ref. 5), and with boundary layers (ref. 6). The mathematical implications of, and a technique for determining this optimum impedance have been reported (refs. 7 and 8). A complete correlation of the optimum point for arbitrary spinning modes in a circular duct with uniform flow is included in this paper.

With this well established optimum point as an input to the approximate attenuation equation, the liner attenuation at any other wall impedance can be calculated. The model is used to generate illustrative examples which provide insight into the operation of acoustic suppressors. Design tools or "rules of thumb" are also generated for the peak spectral attenuation and the attenuation bandwidth.

SYMBOLS

B_θ	optimum resistance coefficient
B_χ	optimum reactance coefficient
b	resonator backing depth, m
C	speed of sound, m/sec
D	circular duct diameter, m
ΔdB	sound power attenuation, dB
ΔdB_m	maximum possible sound power attenuation which is a function of frequency and other variables, dB
ΔdB_{mp}	value of ΔdB_m at the frequency of peak sound attenuation, dB
ΔdB_p	peak value of sound power attenuation
F	function of maximum possible attenuation (see eq. (8))
f	frequency, Hz
f_p	frequency of peak spectral attenuation, Hz
f_1	upper frequency at which half of peak attenuation is attained, Hz
f_2	upper frequency at which half of peak attenuation is attained, Hz
i	$\sqrt{-1}$
L	acoustically treated duct length, m

M_0	uniform steady flow Mach number in duct
m	spinning mode lobe pattern number
Q	$1 + iM_0(\sigma + i\tau)$
R	amplitude of eigenvalue α
$\mathcal{R}$	radius of constant attenuation contour in wall impedance plane
r_0	circular duct radius, m
α	complex eigenvalue ($\alpha = Re^{i\varphi}$)
$\alpha_{m,\mu}$	complex eigenvalue for mode with m circumferential lobes of radial order μ
β	ratio of maximum possible to actual sound power attenuation at a particular frequency
β_p	value of β at the frequency of peak attenuation
γ	$dB_m/dB - 1$ or $\beta - 1$
δ	boundary layer thickness, m
η	frequency parameter, fD/C
η_p	η at the frequency of peak attenuation
θ	specific acoustic resistance
θ_c	resistance coordinate of the center of an equal attenuation or damping contour in the specific acoustic impedance plane
θ_m	optimum specific acoustic resistance which is a function of frequency and other variables
θ_{mp}	value of θ_m at the frequency of peak sound attenuation
μ	radial mode number
ξ	normalized frequency, f/f_p
σ	attenuation coefficient
σ_m	maximum possible value of σ for given set of conditions
τ	propagation coefficient
φ	phase of eigenvalue α
χ	specific acoustic reactance

χ_c reactance coordinate of the center of an equal attenuation or damping contour in the specific acoustic impedance plane

χ_m optimum specific acoustic reactance which is a function of frequency and other variables

χ_{mp} value of χ_m at the frequency of peak sound attenuation

ω circular frequency, rad/sec

DEVELOPMENT OF THE APPROXIMATE EQUATION

The approximate equation that will be presented for the equal damping contours was suggested by the shape of these contours as shown in figure 1. The solid line contours represent exact calculations for a plane wave input into the acoustic liner (ref. 5). Although the contours are quite irregular for high attenuation they become more nearly circular as the attenuation is reduced. Even for high attenuations, a circular contour would usually be sufficient for first approximations. Notice that, as the attenuation is reduced, the center of the contours move to higher resistance. All contour plots seem to show this behavior. Results for spinning modes in ducts with sheared flow will be presented later in this paper. Also shown on figure 1 are the results calculated from Morse's approximate equation which is valid for nearly hard walls or for very low attenuations (less than 10 dB attenuation for the conditions of fig. 1). If this system of circular contours (Morse's approximate results) could be shifted up and to the left, perhaps an adequate approximation to the exact calculations could be achieved even near the optimum impedance. This impedance shift of the circular contours is exactly what the approximate expressions of this paper are intended to accomplish.

Approximate Equation of Morse

The approximate sound attenuation expression, representing the dashed contours of figure 1, which is valid for a plane wave entering a circular duct with nearly hard walls (low attenuation) is given by (ref. 1)

$$\Delta dB \approx \frac{17.4\,\theta(L/D)}{(\theta^2 + \chi^2)} \tag{1}$$

where ΔdB is the sound power attenuation in decibels, θ and χ are the liner

specific acoustic resistance and reactance, L is the length of acoustic treatment, and D is the diameter of the circular duct. The no-flow ($M_0 = 0$) condition is represented by equation (1). Attenuation is understood here and the usual minus sign is omitted. Equation (1) can also be written

$$\left(\theta - \frac{8.7\ L/D}{\Delta dB}\right)^2 + \chi^2 = \left(\frac{8.7\ L/D}{\Delta dB}\right)^2 \tag{2}$$

which represents a system of circular contours with the centers located at

$$\theta_c = \frac{8.7\ L/D}{\Delta dB} \tag{3}$$

$$\chi_c = 0 \tag{4}$$

and of radius

$$\Re = \frac{8.7\ L/D}{\Delta dB} \tag{5}$$

Notice that the approximate expressions already have some of the properties noted in the exact calculations: as the attenuation is reduced the center of the circle moves to higher resistance (θ_c) and the radius ($\Re$) increases.

Improved Approximate Equation

When making the translation of the approximate equal damping contours in the impedance plane, certain restrictions are set upon the equations.

(1) As the maximum possible attenuation is approached the contour radius must approach zero.

(2) At very low attenuations the results should approach equation (1) which is known to be valid for low attenuations.

(3) The contour radius must always be less than the resistance ordinate of the circle center (negative θ's not allowed).

A simple system of equations which satisfies the above restrictions is

$$\theta_c = \theta_m + F\gamma \tag{6}$$

$$\Re = \frac{\theta_m \gamma}{1 + \gamma} + F\gamma \tag{7}$$

where θ_m is the optimum resistance and where

$$F = \frac{8.7\ L/D}{\Delta dB_m (1 + M_0)^2} \tag{8}$$

and

$$\gamma = \frac{\Delta dB_m}{\Delta dB} - 1 \tag{9}$$

with the subscript m on ΔdB_m implying the maximum possible attenuation for the given conditions. Equations (6) to (9) can then be used in

$$(\theta - \theta_c)^2 + (\chi - \chi_m)^2 = \mathcal{R}^2 \tag{10}$$

to provide a reasonable estimate to the exact calculations. The above results were obtained by fitting θ_c and $\mathcal{R}$ to the results obtained from figures 4 and 5 of reference 3 with the Mach number correction determined from reference 5. Note that a plane wave incident upon a soft walled section may produce several modes in the suppressor. The energy balance between, and the effect upon overall sound attenuation of, these modes depend upon the frequency, duct size (L and D), and the wall impedance. These approximate expressions (eqs. (6) to (10)) do not precisely fit the exact calculations over the wide range of conditions considered because of the presence of the several modes. In a later section a more precise expression which is very adequate for single modes will be developed. The behavior of multimodal distributions may then be approximated by repeated use of the single mode equations for several different modes. However, much information has been gained by the use of the cruder expressions given above and the development will proceed with these expressions.

Returning to equations (6) to (10), it is interesting to look at their limits. Note that as $\Delta dB \to \Delta dB_m$, then $\gamma \to 0$, $\theta_c \to \theta_m$, and $\mathcal{R} \to 0$ as required. Also as $\Delta dB \to 0$, $\gamma \approx \Delta dB_m/\Delta dB$ and

$$F\gamma \to \frac{8.7\ L/D}{\Delta dB (1 + M_0)^2} \tag{11}$$

thus

$$\theta_c \to \frac{8.7\ L/D}{\Delta dB (1 + M_0)^2} \tag{12}$$

$$\mathcal{R} \to \frac{8.7\ L/D}{\Delta dB(1 + M_0)^2} \tag{13}$$

and equation (10) becomes

$$\left[\theta - \frac{8.7\ L/D}{\Delta dB(1 + M_0)^2}\right]^2 + (\chi - \chi_m)^2 \approx \left[\frac{8.7\ L/D}{\Delta dB(1 + M_0)^2}\right]^2 \tag{14}$$

which is like equation (2) (when $M_0 = 0$) except for the χ_m term. Thus the result for very small attenuation is like Morse's approximate expression except for the slight shift in reactance.

Notice that all that is now required to completely specify the damping contours throughout the wall impedance plane (using eqs. (6) to (10)) is the optimum resistance (θ_m) and reactance (χ_m) and the maximum possible attenuation (ΔdB_m). Thus off-optimum liner performance can be estimated using only the optimum properties and the liner impedance behavior. These optimum properties will be specified in a later section.

The inverse problem is often of interest: given the resistance and reactance of an acoustic liner, what is the damping? Equations (6), (7), and (10) can be combined to give

$$\theta^2 - 2\theta(\theta_m + F\gamma) + (\chi - \chi_m)^2 + \frac{\theta_m}{(1 + \gamma)}\left[\theta_m \frac{(1 + 2\gamma)}{(1 + \gamma)} + 2F\gamma\right] = 0 \tag{15}$$

If the damping ratio is defined as

$$\beta = \frac{\Delta dB_m}{\Delta dB} = \gamma + 1 \tag{16}$$

then equation (15) is

$$\theta^2 - 2\theta\theta_m - 2\theta F(\beta - 1) + (\chi - \chi_m)^2 + \theta_m\left[\theta_m \frac{(2\beta - 1)}{\beta^2} + \frac{2F(\beta - 1)}{\beta}\right] = 0 \tag{17}$$

Note that to solve for attenuation (ΔdB), β must first be determined from equation (17) which is cubic in β. Instead of using a closed form (but complicated) cubic equation technique, a procedure taking increments in β was used (starting with $\beta = 1$) until equation (17) was satisfied. Approximate solutions to equation (16) or (17) can also be derived for small γ or large β, respectively. For example, when β is large,

$$\beta \approx \frac{\theta^2 - 2\theta\theta_m + 2\theta F + 2\theta_m F + (\chi - \chi_m)^2}{2\theta F} \tag{18}$$

or

$$\Delta dB \approx \frac{17.4\,\theta(L/D)}{\left[\theta^2 - 2\theta\theta_m + 2\theta F + 2\theta_m F + (\chi - \chi_m)^2\right](1 + M_0)^2} \tag{19}$$

which provides a considerable improvement over equation (1).

INPUTS REQUIRED FOR THE APPROXIMATE ATTENUATION EQUATION

In this section the inputs required for the approximate attenuation equations will be presented. These are intended mainly for the single mode equations developed later in the paper. For the simpler equations of the previous section (plane wave) the inputs will be developed as they are used in the next section.

Inspection of equations (8), (16), and (17) shows that M_0, L, D, ΔdB_m, θ_m, and χ_m must be specified before the approximate equations can be used to calculate ΔdB. Also the frequency is necessary to determine the frequency parameter

$$\eta = \frac{fD}{c} \tag{20}$$

since ΔdB_m, θ_m, and χ_m are functions of η. M_0, L, D, and η will be quite easily determined since they will be dictated by the mass flow, size, and frequency of the noise source and the allowable duct length. The results which follow have been determined by empirical correlations of the optimum resistance, reactance, and eigenvalues obtained from exact but tedious calculations involving single mode solutions with lobe number from 1 to 20 and up to the tenth radial mode. The eigenvalues will be used to calculate maximum possible attenuation (ΔdB_m). Circular ducts without centerbodies are considered here.

The optimum resistance and reactance are determined from (ref. 5)

$$\theta_m = B_\theta Q^2 \eta \tag{21}$$

and

$$\chi_m = -B_\chi Q^2 \eta \tag{22}$$

where

$$Q = 1 + iM(\sigma + i\tau) \tag{23}$$

$$\sigma + i\tau = \frac{iM_0 + i\sqrt{1 - \left(1 - M_0^2\right)\left(\frac{\alpha}{m}\right)^2}}{1 - M_0^2} \tag{24}$$

with σ and τ representing the damping and propagation coefficients of the mode (part of the complex wave number) and the eigenvalue is

$$\alpha = Re^{i\varphi} \tag{25}$$

The optimum resistance and reactance coefficients (B_θ and B_χ) will be presented below. Double subscripts (indicating specific modes) have been left off for brevity (on θ_m, χ_m, B_θ, B_χ, Q, σ, τ, and α) but it must be recognized that we are considering a particular mode in the correlations given here. For instance, α should really be considered as $\alpha_{m,\mu}$ where m is the circumferential mode number and μ is the radial mode number. Using this more complete notation, the eigenvalue correlations can be expressed as

$$R_{m,\mu} \approx R_{m,1} + (\mu - 1)\pi + 0.076\, m\sqrt{\mu - 1} \tag{26}$$

$$\varphi_{m,\mu} \approx \varphi_{m,1} e^{\frac{-(\mu-1)}{2(\sqrt{\mu}+m/7)}} \tag{27}$$

where

$$R_{m,1} \approx m + 2.247\, m^{1/3} + 1.521\, m^{-1/3} \tag{28}$$

and

$$\varphi_{m,1} \approx \frac{35.15}{(m+2)^{0.6}} \tag{29}$$

Equation (28) is good for $m \neq 0$. If $m = 0$, use $R_{0,1} = 3.278$. The resistance and reactance coefficients can be estimated from,

$$B_\theta \approx \frac{1.15}{\mu\left(1 + \frac{0.78\ m^{2/3}}{\mu^{3/4}}\right)} \tag{30}$$

$$B_\chi \approx \frac{0.92}{\mu(\mu + 3.17\ m^{2/3})} \tag{31}$$

Note that equations (26) to (31) are valid only at the optimum impedance which is the only input point needed for the approximate attenuation equations. Finally the maximum possible attenuation is calculated from

$$\Delta dB_m = 17.4\ \pi\sigma_m(L/D) \tag{32}$$

where again attenuation being understood, the minus sign has been dropped and the subscript on sigma signifies maximum possible attenuation coefficient.

If equations (25) to (29) are used with $\mu = 1$ to define the eignevalue, and equation (24) is used to calculate the damping coefficient (σ_m), then equation (32) will provide an approximate reproduction of figure 5 in reference 5 for the damping of the least attenuated spinning mode.

A correction may be required for the optimum resistance and reactance in inlets if the boundary layer thickness is significant. This correction is correlated in reference 6 for well cut-on modes. By well cut-on it is implied that

$$\left(1 - M_0^2\right)\left(\frac{\alpha}{\pi\eta}\right)^2 << 1 \tag{33}$$

For modes that are approaching cut-off, a boundary layer refraction correlation has not yet been developed. However as cut-off is approached, the wave fronts travel more transverse to the velocity gradients and the refraction effects should be reduced.

The correlations given in this section are mainly intended to be used with the improved single mode approximate attenuation expressions developed later in this paper. In the next section where plane wave inputs are considered, even more simplified approximations will be used.

SAMPLE CALCULATION - PEAK ATTENUATION AND BANDWIDTH

Illustrative Example

Before the calculations for peak attenuation and bandwidth are made, it is instructive to illustrate the frequency dependent behavior of the equal attenuation contours and of a typical liner impedance. Such an illustration is shown in figure 2 where the attenuation contours are shown for three frequencies each an octave apart. The properties of the optimum points shown here imply well cut-on behavior for all three frequencies. These properties evolve from equations (20) to (22) which show that

$$\theta_m \propto f \tag{34}$$

$$\chi_m \propto -f \tag{35}$$

and equations (24) and (32) which show that (see ref. 5)

$$\Delta dB_m \propto 1/f \tag{36}$$

The optimum points are shown as plus signs; and these, as well as the equal damping contours, are labeled with their relative attenuations. Superimposed upon the damping contours are some sample liner resistances and reactances. These liner impedance loci assume that the resistance (θ) is constant with frequency while the reactance of a Helmholtz resonator at low frequencies behaves as

$$\chi \propto -1/f \tag{37}$$

which implies that back cavity stiffness is controlling the reactance.

First consider the lower resistance locus (open symbols) which pass through the optimum point at the center frequency. As frequency increases the liner impedance moves to the right toward less negative reactance (eq. (37)) while the optimum point and its related contours move to the upper left toward more positive resistance (eq. (34)) and more negative reactance (eq. (35)). As long as the reactance is to the left of its associated optimum (remember that each liner impedance point and each contour set have a frequency associated with them) the damping is increasing with frequency as ever higher damping contours are being cut. When the reactance moves to the right of its associated contour set the damping will fall off and when $\chi = \chi_m$ the peak damping will occur. An example will illustrate these points. At $f = 1/2\ f_p$ the far left wall impedance point

($\theta = 1$, $\chi = -2$) is associated with the contours centered at the lower right and a relative damping of 0.52 dB is obtained. At $f = f_p$, the liner impedance is coincident with the optimum point of the center contour set and a relative damping of 1 dB is obtained. For the far right liner impedance (1, -0.5) at $f = 2f_p$ use the contour set centered at the upper left to read 0.19 dB. In this example three points have been established in the sound attenuation spectrum. More points could be similarly determined at other frequencies.

Now if this exercise is repeated at a higher resistance of $\theta = 3$ shown by the solid symbols in figure 2 it is seen that the liner impedance never passes through an optimum impedance point but the relative damping still has a relative peak at the center frequency where $\chi = \chi_m$. Table I reviews the above results with an intermediate resistance also included.

Note that a modest increase in resistance ($\theta = 1.6$) above the optimum causes the peak damping to be reduced only moderately while both the high and low frequencies have improved attenuation. A further increase in resistance ($\theta = 3$) improves the higher frequency damping but decreases the damping at both of the other frequencies. Further increases in resistance would result in falloff of attenuation at all frequencies. The trade-off between peak attenuation and bandwidth would be determined by the specific application being studied.

An exact calculation using the wave equation and more exact liner properties would be performing the same ritual as illustrated in figure 2 except that the significance of the visualization would be lost in the process. A more sophisticated approach would use many modes at a time meaning that multiple contour sets would be considered simultaneously.

Equations and Approximations

In this section the peak attenuation and the attenuation bandwidth with a plane wave input are determined to provide one illustration of the use of the approximate attenuation equations. Both quantities are functions mainly of the ratio of actual resistance to the optimum resistance at the peak attenuation frequency. The starting point is equation (17), which when divided by θ_{mp}^2, yields

$$\left(\frac{\theta}{\theta_{mp}}\right)^2 - \frac{2\theta\theta_m}{\theta_{mp}^2} - \frac{2\theta F}{\theta_{mp}^2}(\beta - 1) + \frac{(\chi - \chi_m)^2}{\theta_{mp}^2} + \frac{\theta_m}{\theta_{mp}}\left[\frac{\theta_m(2\beta - 1)}{\theta_{mp}\beta^2} + \frac{2F(\beta - 1)}{\theta_{mp}\beta}\right] = 0 \quad (38)$$

Recall that θ is the suppressor resistance, θ_m is the optimum resistance which

is a function of frequency, and θ_{mp} is the optimum resistance at the frequency of peak attenuation at which $\chi = \chi_m$. In the development which follows (to eq. (43)), some very simplified interrelationships among the quantities in equation (38) will be used. The objective is to reduce equation (38) to a form which gives attenuation (through β) as a function only of a frequency ratio, a resistance ratio, and a peak frequency parameter. Define the quantity

$$\xi = \frac{f}{f_p} \tag{39}$$

where f_p is the frequency at which $\chi = \chi_m$. From equation (20) and (21)

$$\frac{\theta_m}{\theta_{mp}} = \frac{\eta}{\eta_p} = \frac{f}{f_p} = \xi \tag{40}$$

where it was assumed that Q^2 is not a function of frequency, which implies that either $M_0 = 0$ (then $Q = 1$), or that the frequencies involved are all above cut-off leading to $Q = 1/(1 + M_0)$ (see ref. 5). Let the reactance be controlled by the back cavity

$$\chi \approx -\cot\frac{\omega b}{c} \approx -\frac{c}{2\pi bf} \tag{41}$$

where the second approximation is valid for small arguments of the cotangent, and where b is the liner backing depth. Also

$$\chi \approx -\frac{c}{2\pi bf_p}\frac{f_p}{f} = \frac{\chi_{mp}}{\xi} \tag{42}$$

where equation (41) was used to define χ_{mp} as χ at $f = f_p$. Equations (21) and (22) yield

$$\chi_m = -\frac{B_\chi \theta_m}{B_\theta} \approx -\frac{\theta_m}{3} \tag{43}$$

where $B_\theta \approx 3B_\chi$ is a rough estimate from table I of reference 6 for axisymmetric wave propagation. Then from equations (40), (42), and (43)

$$\frac{(\chi - \chi_m)^2}{\theta_{mp}^2} \approx \frac{\left(1 - \xi^2\right)^2}{9\xi^2} \tag{44}$$

If, instead of using the approximation in equation (41), the cotangent had been retained, the result would be

$$\frac{(\chi - \chi_m)^2}{\theta_{mp}^2} \approx \left\{ \frac{-1}{\eta_p \tan\left[\xi \tan^{-1}\left(\frac{3}{\eta_p}\right)\right]} + \frac{\xi}{3} \right\} \tag{45}$$

An approximation to the maximum possible attenuation results of reference 3 can be expressed as,

$$\frac{\Delta dB_m}{L/D} \approx \frac{65}{\left(1 + 38\,\eta^4\right)^{1/4}} \tag{46}$$

Finally using equations (8), (21), and (46)

$$\frac{F}{\theta_{mp}} = \frac{\left(1 + 38\,\eta_p^4 \xi^4\right)^{1/4}}{7.5\,\eta_p} \tag{47}$$

where $B_\theta \approx 1$ and $Q \approx 1/(1 + M_0)$ were used. For sufficiently high frequencies (high $\eta_p \xi$)

$$\frac{F}{\theta_{mp}} \approx \frac{\xi}{3} \tag{48}$$

Inserting equations (40) and (44) into (38) yields,

$$\left(\frac{\theta}{\theta_{mp}}\right)^2 - 2\left(\frac{\theta}{\theta_{mp}}\right)\xi - 2\left(\frac{\theta}{\theta_{mp}}\right)\left(\frac{F}{\theta_{mp}}\right)(\beta - 1) + \frac{\left(1 - \xi^2\right)^2}{9\xi^2}$$

$$+ \xi\left[\xi\,\frac{(2\beta - 1)}{\beta^2} + 2\left(\frac{F}{\theta_{mp}}\right)\frac{(\beta - 1)}{\beta}\right] = 0 \tag{49}$$

Equation (49) along with (47) or (48) (depending upon $\eta_p \xi$ or frequency) can be used in two ways. First with $\xi = 1$ the peak attenuation was calculated through β_p as a function mainly of θ/θ_{mp}. The inverse of β_p ($\Delta dB_p/\Delta dB_{mp}$) determined from equation (49) is plotted in figure 3. For liner resistance below the

optimum resistance, a single curve is obtained for all frequency parameters (η_p) and the result is

$$\Delta dB_p = \frac{\theta}{\theta_{mp}} \Delta dB_{mp}; \quad (\theta < \theta_{mp}) \tag{50}$$

a conveniently simple expression. Equation (49) can be seen to contain the factor ($\beta - \theta/\theta_{mp}$) when $\xi = 1$, which accounts for this simple relationship.

For liner resistance above the optimum the peak attenuation is seen to be a weak function of frequency parameter (η_p). An adequate approximation is,

$$\Delta dB_p \approx \frac{\theta_{mp}}{\theta} \Delta dB_{mp}; \quad (\theta > \theta_{mp}) \tag{51}$$

These two relationships, equations (50) and (51), are extremely useful "rules of thumb" in preliminary suppressor design considerations and in interpretation of acoustic liner data.

Some results of exact calculations obtained from reference 3 are included on figure 3 for comparison with the approximate results obtained from equation (49).

The second use of equation (49) was to fix β at some desired level and determine the frequency ratio ($\xi = f/f_p$) at which this attenuation occurred. This was done to determine the attenuation bandwidth or the frequencies at which $\Delta dB = 1/2\ \Delta dB_p$, for instance. This can be accomplished by the following. Let

$$\Delta dB = 1/2\ \Delta dB_p \tag{52}$$

then

$$\beta = \frac{\Delta dB_m}{\Delta dB} = \frac{\Delta dB_p}{\Delta dB} \frac{\Delta dB_{mp}}{\Delta dB_p} \frac{\Delta dB_m}{\Delta dB_{mp}} = 2\beta_p \frac{\Delta dB_m}{\Delta dB_{mp}} \tag{53}$$

Use of equation (46) gives,

$$\frac{\Delta dB_m}{\Delta dB_{mp}} \approx \left(\frac{1 + 38\eta_p^4}{1 + 38\eta_p^4 \xi^4} \right)^{1/4} \approx \frac{1}{\xi} \text{ (for large } \eta_p \xi) \tag{54}$$

The lower and upper frequencies (f_1/f_p and f_2/f_p) for which one-half peak attenuation occurs were calculated with both representations of the reactance (eq. (41)). The results are shown in figures 4 and 5 with all of the calculations

made with the cotangent representation of reactance except for the curves labeled "large η_p limit, lumped reactance." For large η_p the cotangent representation approaches the lumped reactance result. The breakaway from the "lumped reactance" curve for $\theta/\theta_{mp} > 1$ in figure 5 occurs where the back cavity half wave frequency is being approached, the reactance is approaching infinity and the attenuation is going to zero. In a real liner where a high damping resonator is used this cannot occur and the use of the lumped reactance curve is probably more nearly correct for constructing the attenuation spectrum. Some fall off in attenuation will be anticipated beyond this half wave point.

Some interesting conclusions can be seen from figures 4 and 5. For liner resistance below the optimum ($\theta/\theta_{mp} < 1$) bandwidth remains essentially constant since f_1/f_p and f_2/f_p do not change much. Recall from figure 3 that peak attenuation falls off as resistance is reduced below the optimum. Thus no improvement in liner performance is gained from underdamping the liner. However, for high resistance ($\theta/\theta_{mp} > 1$), although peak attenuation is lost, bandwidth is gained since f_1/f_p is reduced and f_2/f_p is increased. Recall from the discussion of figure 2 that increasing the resistance above the optimum value to improve attenuation bandwidth can be pushed too far since at very high resistance the entire attenuation spectrum will be reduced as resistance is increased.

Some useful "rules of thumb" can also be determined for bandwidth. These are obtained from observation of the results in figures 4 and 5. For resistances below the optimum,

$$f_1/f_p \approx f_1/f_p)_{opt} \tag{55}$$

$$f_2/f_p \approx f_2/f_p)_{opt} \tag{56}$$

For resistance above optimum

$$f_1/f_p \approx \frac{\theta_{mp}}{\theta} f_1/f_p)_{opt} \tag{57}$$

$$f_2/f_p \approx \frac{\theta}{\theta_{mp}} f_2/f_p)_{opt} \tag{58}$$

The subscript opt implies the condition when $\theta = \theta_{mp}$. The following correlations are offered at the optimum resistance for use with equations (55) to (58). These were obtained by plotting the results at $\theta/\theta_{mp} = 1$ from figures 4 and 5 against η_p.

$$f_1/f_p)_{opt} \approx \frac{1 + 0.56\,\eta_p^{3/2}}{1 + 1.6\,\eta_p^{3/2}} \tag{59}$$

$$f_2/f_p)_{opt} \approx \frac{1 + 4.21\,\eta_p^{2}}{1 + 3.05\,\eta_p^{2}} \tag{60}$$

Although the sample calculations made here used information about circular duct optima, the final results (peak attenuation and bandwidth "rules of thumb") would be expected to apply to other geometries as well. For other geometries only the constants (such as B_θ, B_χ, ΔdB_m) in the problem would change. The key behavior of the approximate attenuation contours would not change. This behavior includes the unsymmetrical shape of the contour pattern, the movement of the contours in the impedance plane as frequency changes, and the fall-off in ΔdB_m as frequency increases. One precaution must be observed, however, and that is in the use of equations (59) and (60). The frequency parameter at peak attenuation (η_p) must be considered relative to the cut-off frequency parameter. For example when $\eta_p = 1$, cut-off is approached in the example shown. For smaller values of η_p, ΔdB_m approaches a constant (losing the $1/f$ dependence). For the first radial mode of a 20-lobe spinning pattern in a circular duct, ΔdB_m versus η will flatten out below $\eta = 10$ (see ref. 5).

The three quantities calculated here (ΔdB_p, f_1, and f_2) can be used to obtain a first approximation to the attenuation spectrum. Log ΔdB versus log f is used with straight lines connecting the three points to obtain a reasonable approximation to the attenuation spectrum. Of course, the entire attenuation spectrum could be calculated from the approximate attenuation equations by using a multitude of frequencies rather than just f_1, f_p, and f_2.

These simplified notions about peak attenuation and bandwidth have been used to analyze the attenuation data for inlet suppressors with splitter rings mounted on full scale fans and engines. These results are reported in reference 9 and show fairly good agreement between theory and data. Splitter ring suppressors seem to be relatively insensitive to spinning mode content (ref. 5) and can be adequately described using the least attenuated radial mode.

IMPROVED SINGLE MODE APPROXIMATE ATTENUATION EQUATION

Due to the form of the approximate attenuation equations discussed in this paper, the attenuation is assured of being an accurate representation of the more

exact propagation calculations at the extremes of damping. At the optimum impedance the attenuation will become the maximum possible and far from the optimum impedance the attenuation will approach zero. Between these extremes a good fit to exact calculations was obtained by the empiricism inserted in the approximate equations. As discussed previously, a plane wave input to a soft walled duct leads to a multimodal solution in the soft duct. The balance among the modes in determining the overall attenuation depends upon the wall impedance, the frequency and the liner geometry. A good fit of the approximate equations to the exact calculations cannot be made over all conditions. A better approach is to use approximate equations for each mode and to build up the total solution from the component parts. An improved single mode solution to provide the basis for such an approach will now be developed.

The resistance coordinate for the circular contour center was not altered,

$$\theta_c = \theta_m + F\gamma = \theta_m + F(\beta - 1) \tag{6}$$

but the radius has been changed to,

$$\mathcal{R} = \frac{\theta_m \gamma^2}{(\gamma + 1)(\gamma + 2)} + F\gamma = \frac{\theta_m (\beta - 1)^2}{\beta(\beta + 1)} + F(\beta - 1) \tag{61}$$

In addition, the reactance coordinate for the center of the constant attenuation contours can be represented as,

$$\chi_c = \frac{\chi_m}{\gamma + 1} = \frac{\chi_m}{\beta} \tag{62}$$

The definition of F has not been altered and is repeated as,

$$F = \frac{8.7\ L/D}{\Delta dB_m (1 + M_0)^2} \tag{8}$$

Technically the definition of F should have been altered since the solution for nearly hard walls results in,

$$\theta_c \text{ and } \mathcal{R} \to \frac{8.7\ \alpha_\infty^2\ L/D}{\Delta dB (1 + M_0)^2 \left(\alpha_\infty^2 - m^2\right)} \tag{63}$$

Where m is the spinning pattern lobe number and α_∞ is the mode eigenvalue for hard walls. Empirically this refinement (using $\alpha_\infty^2/(\alpha_\infty^2 - m^2)$) was found to be unnecessary in any reasonable vicinity of the optimum impedance (attenuations down to 1/50 of the maximum possible) and this term was omitted from the development. For extremely low damping equation (63) might be used with equation (10) (with $\chi_m = 0$) if desired.

Use of equations (6), (61), and (62) in equation (10) (with χ_c replacing χ_m in eq. (10)) yields,

$$\theta^2 - 2\theta\left[\theta_m + F(\beta - 1)\right] + \left(\chi - \frac{\chi_m}{\beta}\right)^2 + \frac{\theta_m(3\beta - 1)}{\beta(\beta + 1)}\left[\frac{\theta_m(2\beta^2 - \beta + 1)}{\beta(\beta + 1)} + 2F(\beta - 1)\right] = 0 \qquad (64)$$

For circular ducts, the inputs (θ_m, χ_m, ΔdB_m) can be calculated from the results given in a previous section (INPUTS REQUIRED FOR THE APPROXIMATE ATTENUATION EQUATION) and the attenuation (through β) can then be calculated at any resistance (θ) and reactance (χ) using equation (64). This equation is now seen to be of fifth power in β and a stepping or iteration approach must be used. Usually the β denominator of χ_m can be omitted without much loss of accuracy.

The equal attenuation contours (expressed for convenience by the attenuation coefficient σ rather than ΔdB, see eq. (32) for relationship) of the improved single mode approximate equation are compared to the exact calculations for a seven lobe spinning wave in figures 6 and 7. Figure 6 illustrates the first radial while figure 7 is for the fifth radial mode. The agreement between the approximate and exact calculations is seen to be quite good in both cases. The first radial mode would be considered well cut-on while the fifth radial is approaching cut-off (the left hand side of eq. (33) is ≈ 0.46 which is not much less than 1). The rotation of equal attenuation contours which occurs in the wall impedance plane due to Q^2 in equations (21) and (22) has been accounted for and the entire contour pattern rotates with the optimum point. The exact equal damping contours of figures 6 and 7 were calculated as in reference 6 using a fairly thin boundary layer. Note the exact contours are tear-drop shaped for the higher attenuations but rapidly approach circular shape as the damping of the contours is reduced. The shift of the equal contour centers toward higher resistance as damping decreases is much more obvious in figures 6 and 7 than in figure 1.

CONCLUDING REMARKS

Many equal damping contour plots have been investigated beyond the three that have been presented in this paper. These include a wide range of spinning lobe numbers and radial mode numbers, both with and without steady flow boundary layers. All of these plots seem to have the behavior described in this paper. The contours are nearly circular with the centers of these circles moving to higher resistance as the attenuation of the contour is reduced.

With the contour properties and Morse's approximate equation as guides, the approximate attenuation equations were developed. Two versions of the approximate equations were presented. The first version has some contour broadening due to the multimodal nature of the exact solution to which it was fit. The second version, which is the favored version for future use, was generated to fit single modes only. As a result this version is a more accurate representation of more exact calculation procedures.

Although the approximate attenuation equation was presented only as an alternate to more time consuming exact calculation procedures, such approximate solutions may represent the most sensible approach for acoustic liner design. Due to the unknown nature of the modal input to be used and the possible errors in physically obtaining the desired (analytical) value of wall acoustic impedance, it is possible that exact wave equation solutions are not justified.

Using the approximate attenuation equation the following "rules of thumb" were observed.

1. For liner resistance above the optimum, the peak attenuation is inversely proportional to resistance and the attenuation bandwidth increases with resistance.

2. For liner resistance below the optimum, the peak attenuation is reduced proportionally with the resistance but the attenuation bandwidth remains constant.

REFERENCES

1. P. M. Morse, Vibration and Sound, 2nd ed. (McGraw-Hill, New York, 1948).

2. V. Cremer, "Theory of Sound Attenuation in a Rectangular Duct with an Absorbing Wall and the Resultant Maximum Coefficient," Acustica, 3, 249-263 (1958).

3. E. J. Rice, "Attenuation of Sound in Soft-Walled Circular Ducts," in Aerodynamic Noise, H. S. Ribner, ed. (Univ. of Toronto Press, 1969, pp. 229-249).

4. E. J. Rice, "Propagation of Waves in an Acoustically Lined Duct with a Mean Flow," in Basic Aerodynamic Noise Research, NASA SP-207, pp. 345-355 (1969).

5. E. J. Rice, "Spinning Mode Sound Propagation in Ducts with Acoustic Treatment," NASA TN D-7913 (1975).

6. E. J. Rice, "Spinning Mode Sound Propagation in Ducts with Acoustic Treatment and Sheared Flow," AIAA Pap. 75-519 (1975).

7. B. J. Tester, "The Optimization of Modal Sound Attenuation in Ducts, in the Absence of Mean Flow," J. Sound Vib., 27, pp. 477-513 (1973).

8. W. E. Zorumski and J. P. Mason, "Multiple Eigenvalues of Sound-Absorbing Circular and Annular Ducts," J. Acoust. Soc. Am., 55, pp. 1158-1165 (1974).

9. G. L. Minner and E. J. Rice, "Computer Method for Design of Acoustic Liners for Turbofan Engines," NASA TM X-3317.

TABLE I. - RELATIVE DAMPING WITH RESISTANCE AND FREQUENCY

θ	$1/2\ f_p$	f_p	$2f_p$
1	0.52	1	0.19
1.6	.61	.82	.27
3	.51	.57	.35

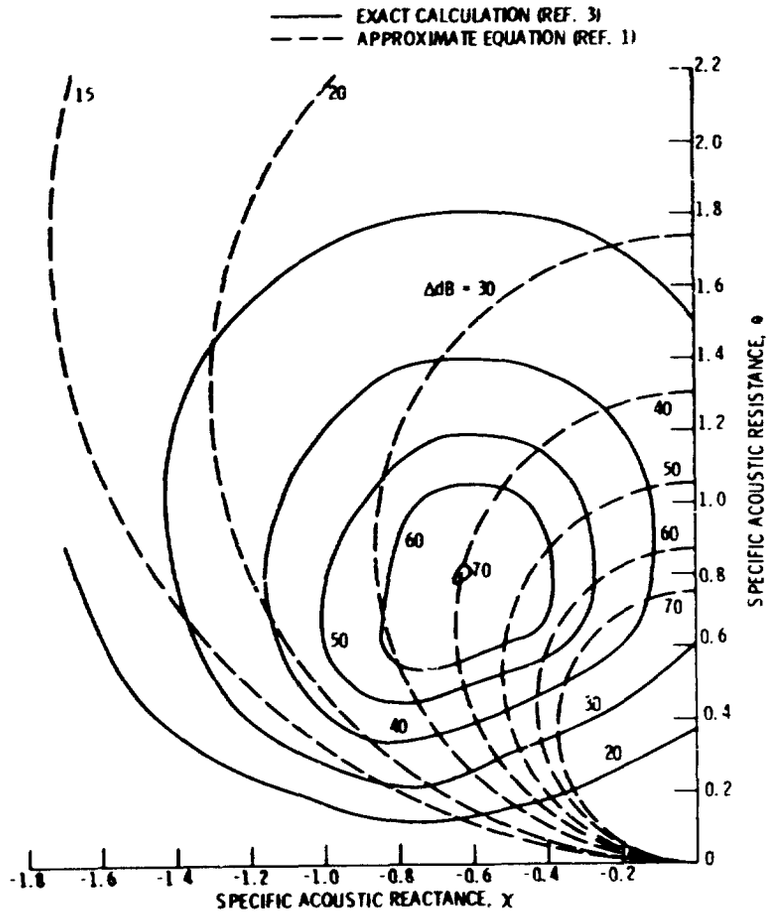

Figure 1. - Sound power attenuation contours for plane wave input, circular duct, zero Mach number, frequency parameter η = 1, duct length to diameter ratio L/D = 3.

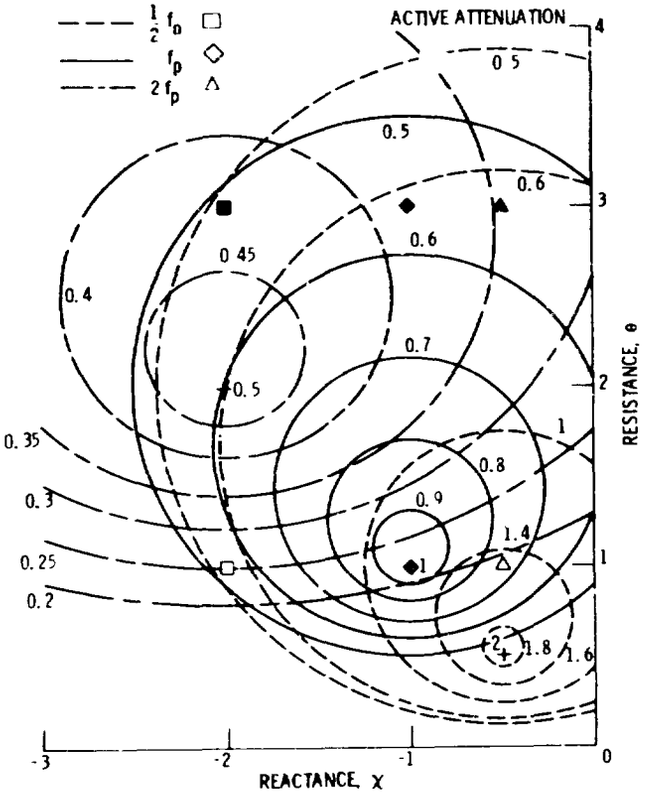

Figure 2. - Illustration of equal damping contours for three different frequencies.

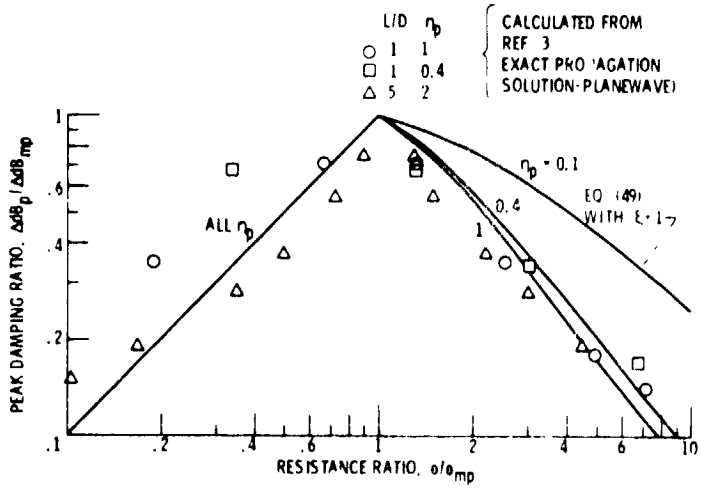

Figure 3. - Variation of peak attenuation with liner resistance.

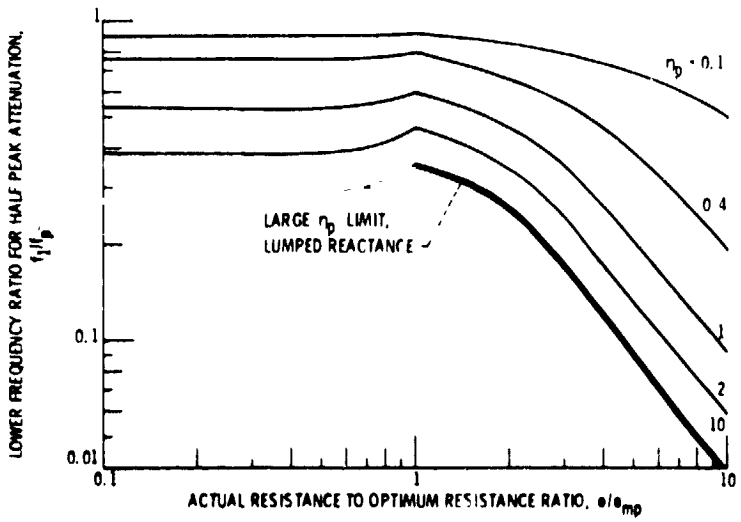

Figure 4. - Lower bandwidth frequency related to liner resistance.

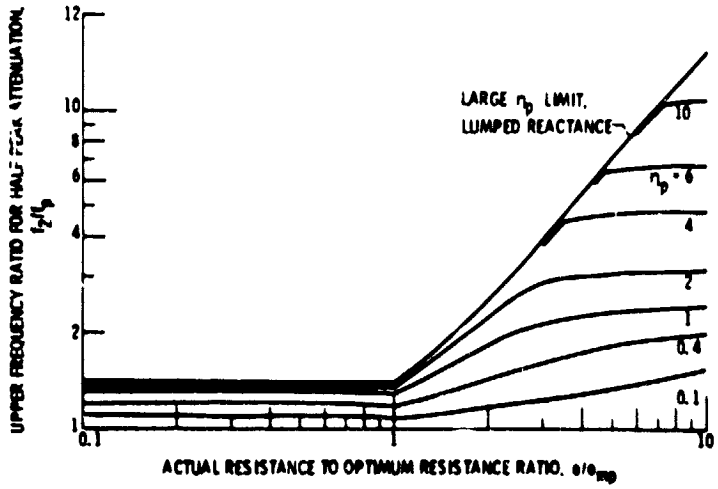

Figure 5. - Upper bandwidth frequency related to liner resistance.

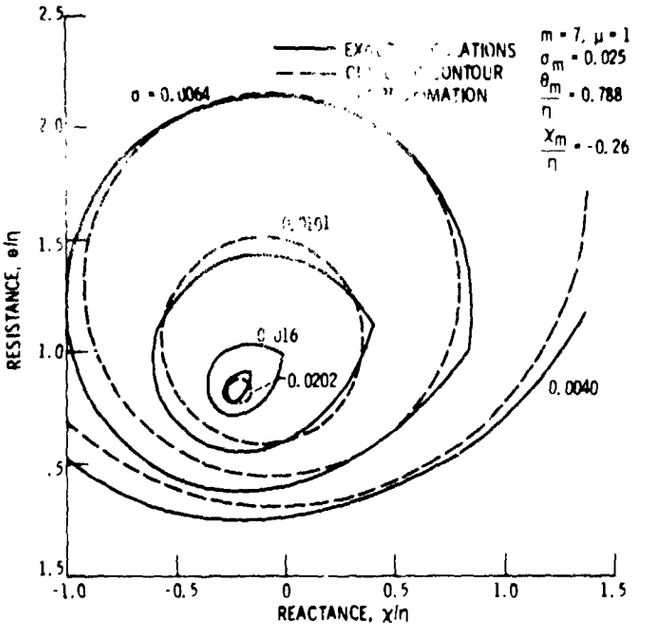

Figure 6. - Equal damping contours for seventh circumferential, first radial mode (m = 7, μ = 1), Mach number M_0 = -0.4, frequency parameter η = 10, boundary layer to radius ratio δ/r_0 = 0.002.

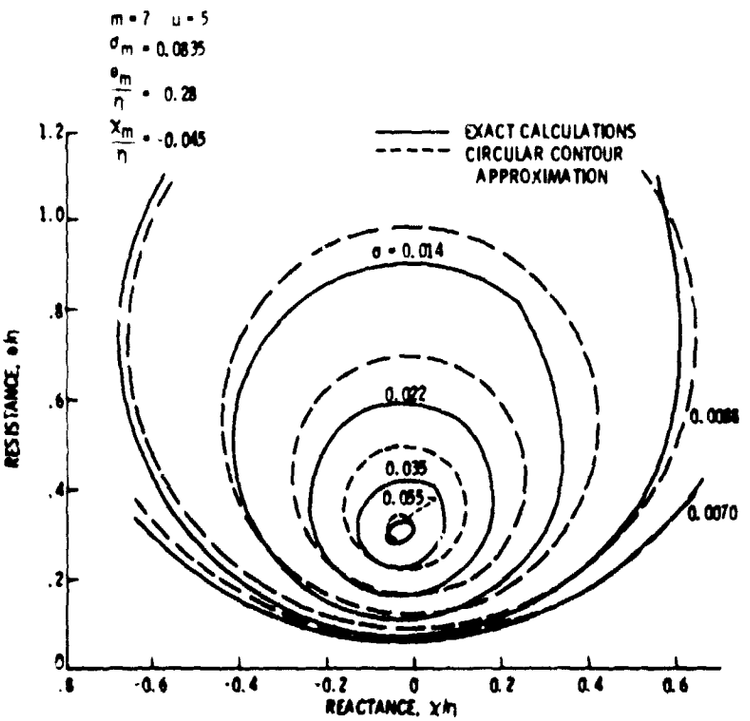

Figure 7. - Equal damping contours for the seventh circumferential, fifth radial mode (m = 7, μ = 5), Mach number M_0 = -0.4, frequency parameter η = 10, boundary layer to radius ratio δ/r_0 = 0.002.